

Radar Absorber Fabric Design Based on Periodic Arrays of Circular Shaped Conductive Patches

Muhammet Hilmi Nisancı^{1*} , Baha Kanberoglu¹ , Yılmaz Çiğdem¹ , Fatih Özkan Alkurt² ,
Muharrem Karaaslan² 

¹ Department of Electrical and Electronics Engineering Department, Sakarya University, Sakarya, 54055, Turkey,

² Department of Electrical and Electronics Engineering Department, Iskenderun Technical University, Iskenderun, Hatay, Turkey

* nisanci@sakarya.edu.tr

* Orcid : 0000-0002-8210-7260

Received: 13 April 2021

Accepted: 19 January 2022

DOI: 10.18466/cbayarfbe.915217

Abstract

In this study, the design and electrical tests of polarization-independent radar absorber fabric containing an array of circular shaped conductive patches positioned on a neoprene fabric are presented. The proposed absorber has an overall thickness of 1.57 mm and a unit cell dimension of $8.75 \times 8.75 \text{ mm}^2$, which is $< \lambda/3$, where λ is the free-space wavelength at 9.33 GHz. In the designs, electrical performance of the radar absorber fabric is numerically studied in both planar and conformal structures. Furthermore, the two-dimensional (2D) surface current distribution at the resonant frequency is examined to better understand the operating principles of the proposed structure. Finally, a prototype of the radar absorber is manufactured using neoprene fabric with relative permittivity of 3.18, loss tangent of 0.93, and the frequency dependent reflection parameter values are measured by using the free space measurement technique to validate the numerical results. A good agreement between the measurement and numerical results is obtained.

Keywords: Radar absorber fabric, metamaterials, frequency selective surfaces.

1. Introduction

Radars are commonly used for detecting, locating, tracking, and recognizing of the air, land and sea vehicles such as ships, aircraft and space crafts for both civilian and military purposes [1]-[4]. Radar Absorbing Materials (RAM) which convert the incident electromagnetic energy into thermal energy should be used to make harder to detect of these vehicles by radars [5]-[7]. The traditional RAMs based on frequency selective surface (FSS) are include periodically arranged of conductive patches located on a dielectric substrate. In the literature various FSS designs with different unit element geometries are proposed to reduce the electromagnetic energy reflected back to the radar [8]-[10].

In [11], a thin absorber which consists of a single resistive FSS layer and a dielectric superstrate is designed to operate in the frequency range of approximately 3.3 to 20 GHz with 88.26% bandwidth. In the designs, square patches are used as the unit cell

elements to simplify the derivation of the equivalent circuit model. The three-layer ultrathin RAM which includes an FSS with double square loops is considered in [12]. In order to improve the absorption performance of the considered structure micro-split gaps are opened in the middle of the outer square loops. In this way, the -10dB absorption bandwidth is increased to 14.1 GHz. Another design is shown in [13], where a tunable circuit analog absorber is proposed for the first time. The basic idea of the tunable circuit analog absorbers is replacing the conventional ground plane by a varactor tunable FSS. The RAMs can be also used for conformal surface applications. For this purpose, in [14], a Jaumann absorber with a low-pass FSS back layer is applied to the curved wing-front end to efficiently reduce the monostatic radar cross-section for both TE and TM polarizations over 2–16 GHz.

Recently fabric-based radar absorbers are becoming more popular for their low processing cost, flexibility, light weight and easy fabrication [15].

In the proposed study a polarization-independent radar absorber fabric is designed to operate in the center frequency of the X-band.

This paper is organized as follows. Section 2 describes the design procedure and numerical analysis of the proposed model. Section 3 details the manufacturing and measurement processes. Moreover, this section compares the measurement results with numerical results in the frequency range of interest. Finally, Section 4 presents the evaluation and conclusions of the paper.

2. Radar Absorber Fabric Design and Operating Principle

In this study, radar absorber fabric design with circular shaped conductive patch array providing polarization-independent absorption characteristic for both TE and TM modes under different incident angles due to the symmetrical shape of the patches is considered. As shown in Figure 1, the proposed structure has four design parameters; the radius of the circular patches r , the thickness of the fabric positioned between the conductive patches t , the side length of the unit element h and the relative permittivity of the fabric positioned between the conductive patches ϵ_r . The design parameter values of the absorber fabric are obtained by using CST Microwave Studio optimization tools for 9.33 GHz center frequency value as listed in Table 1 [16].

Table 1. Design parameter values of radar absorber fabric with circular shaped patch array

Parameter	Description	Value
r	the radius of the circular patches	3 mm
t	the thickness of the fabric positioned between the conductive patches	1.5 mm
h	the side length of the unit element	8.75 mm
ϵ_r	the relative dielectric permittivity of the fabric	3.5

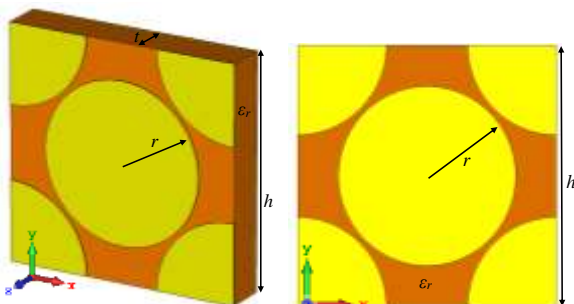


Figure 1. Design parameters of the radar absorber fabric with a circular shaped patch array

In the simulations, the open boundary condition is used along z-direction whereas electric and magnetic boundary conditions are respectively used along the x and y-directions to eliminate all tangential electric and magnetic fields. Furthermore, the unit element model illustrated in Figure 1 is excited with a pure TEM mode by two 50 Ω waveguide ports which are located over xy planes at equal distances from the panel along the z-axis.

The frequency dependent transmission (T), reflection (R) and absorption (A) coefficient values obtained from numerical analysis are compared in Figure 2. It is observed from the comparison given in Figure 2, the amplitude values of the reflection and absorption coefficients are respectively minimum and maximum at the center operating frequency of 9.33 GHz, while the transmission coefficient values are equal to zero throughout the frequency range due the ground plane used in the designs.

$$T + R + A = 1 \quad (2.1)$$

Considering Eq. (1), the sum of the amplitude values of the frequency dependent transmission, reflection and absorption coefficients should be equal to 1. While the transmission parameter values are zero due to the ground plane, the reflection and absorption coefficients should be symmetrical with respect to each other. Therefore, in this study, only reflection coefficient values are taken into consideration in the numerical analysis.

The effect of various incidence angles and polarizations of the electromagnetic wave on the electrical performance of the radar absorber fabric is also considered in this study. For this purpose, numerical analysis is performed for the angle of incidence of the electromagnetic wave between 0° – 60° with 15° angle steps and the obtained frequency dependent reflection parameters are compared in Figure 3.

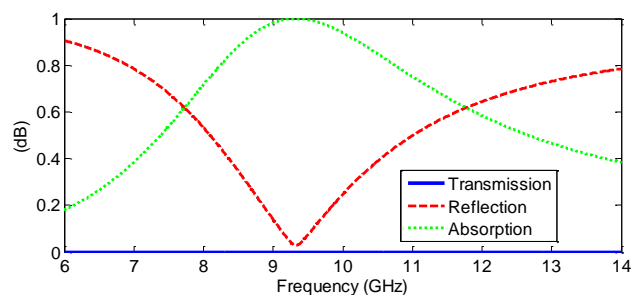


Figure 2. Numerically obtained frequency dependent transmission (T), reflection (R) and absorption (A) coefficient values of the radar absorber fabric

It can be seen from Figure 3 that the operating frequency value of the radar absorber fabric shifts towards higher frequencies depending on the increase in the incidence angle.

To examine the electrical performance of the radar absorber fabric against different polarizations of the electromagnetic wave, the angle of the wave with the x -axis is changed with 15° steps between 0° – 60° and the obtained frequency dependent reflection parameters are compared in Figure 4. From the comparison given in Figure 4, the proposed radar absorber fabric design shows a polarization independent characteristic.

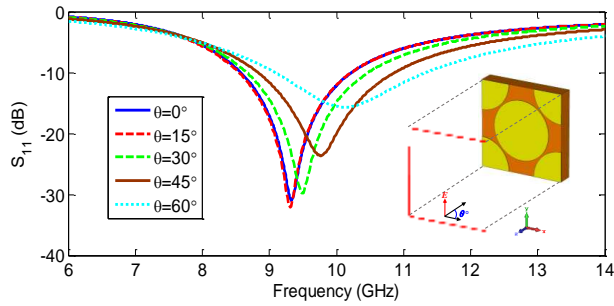


Figure 3. Numerically obtained frequency dependent reflection coefficient values of the radar absorber fabric for various incidence angle of electromagnetic wave

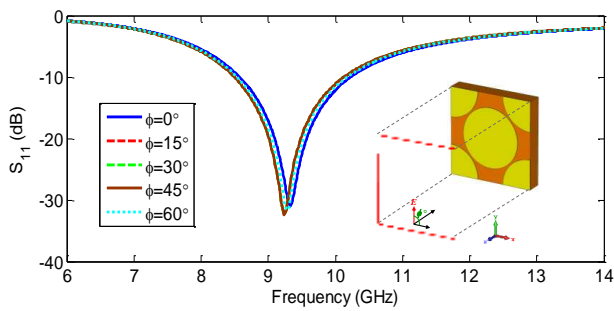


Figure 4. Numerically obtained frequency dependent reflection coefficient values of the radar absorber fabric various polarizations of the electromagnetic wave

In order to investigate the electrical performance of the proposed structure, 2D surface current density at the operating frequency of the radar absorber fabric with normal electromagnetic wave excitation ($\phi=0^\circ$, $\theta=0^\circ$) is considered. As can be clearly seen from Figure 5, conductive circular patches resonate at operating frequency.

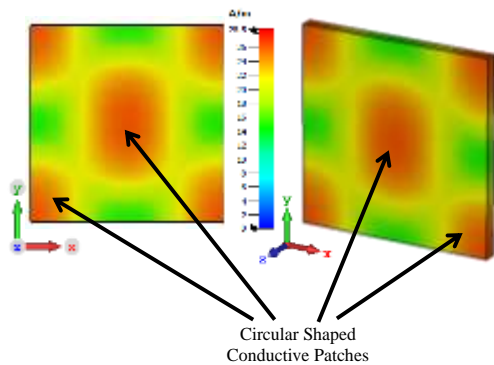


Figure 5. 2D surface current distribution at the center operating frequency of the radar absorber fabric

After the 2D surface current density of the proposed structure is studied, several simulations are implemented to investigate the effect of the design parameter values on the electrical performance of the radar absorber. For this purpose, only one design parameter value is varied while the others are fixed as shown in Table 2.

Table 2. Design parameter values used in the parameter analysis of radar absorber fabric

Model	r	t	h	ϵ_r
Ref. Model	3 mm	1.5 mm	8.75 mm	3.5
Model-1	2.94 mm	1.5 mm	8.75 mm	3.5
Model-2	3.06 mm	1.5 mm	8.75 mm	3.5
Model-3	3 mm	1.3 mm	8.75 mm	3.5
Model-4	3 mm	1.7 mm	8.75 mm	3.5
Model-5	3 mm	1.5 mm	8.55 mm	3.5
Model-6	3 mm	1.5 mm	8.95 mm	3.5
Model-7	3 mm	1.5 mm	8.75 mm	2.5
Model-8	3 mm	1.5 mm	8.75 mm	4.5

The first parameter to be studied is the radius of the circular patches r . As can be clearly seen from Figure 6, the center of the operating frequency moves to 9.86, 9.33, and 8.62 GHz by varying r as 2.94, 3, and 3.06 mm, respectively.

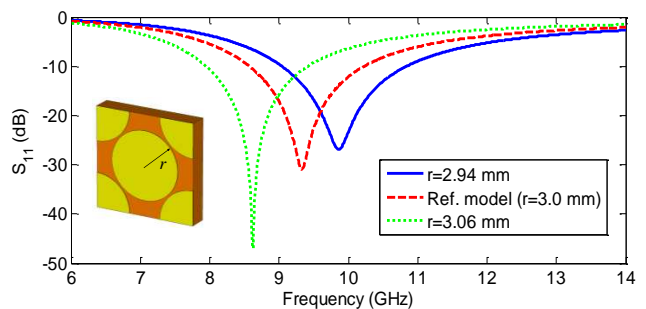


Figure 6. Numerically obtained reflection coefficient results of the proposed radar absorber as the function of the r .

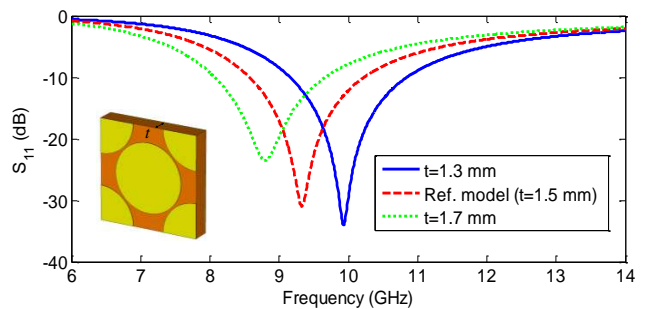


Figure 7. Numerically obtained reflection coefficient results of the proposed radar absorber as the function of the t .

In order to investigate the effect of the thickness of the fabric positioned between the conductive patches and ground plane on the operating frequency, t is varied from 1.3 mm to 1.7 mm with an increment of 0.2 mm. Figure 7 confirms that the operating frequency is inversely proportional to t .

The effect of the unit cell dimension on the reflection coefficient values of the radar absorber fabric is compared in Figure 8 under varying the values of h . As depicted in in Figure 8, the center of the operating frequency values are obtained as 8.55, 9.33, and 9.8 GHz for the unit cell dimension values of 8.55, 8.75, and 8.95 mm, respectively.

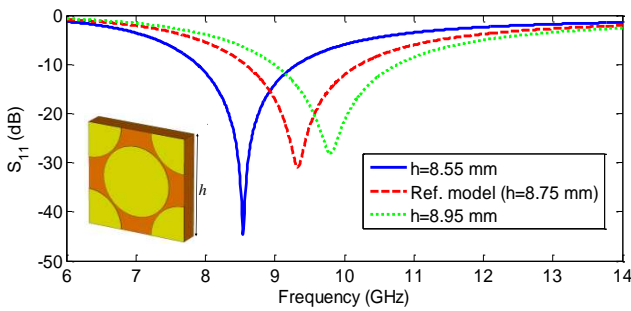


Figure 8. Numerically obtained reflection coefficient results of the proposed radar absorber as the function of the h .

Finally, the effect of the relative dielectric permittivity of the fabric ϵ_r on the electrical performance is considered. According to Figure 9, the operating frequency is inversely proportional to the relative dielectric permittivity value of the fabric.

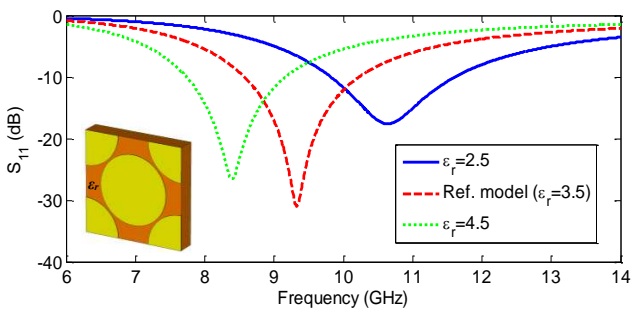


Figure 9. Numerically obtained reflection coefficient results of the proposed radar absorber as the function of the ϵ_r .

Before starting the manufacturing process of the radar absorber fabric, the electrical performance of the absorber fabric on the conformal structures is considered. For this purpose, the designed absorber fabric is placed on a cylindrical conformal structure which has an average inner radius of 8.8 cm as shown in Figure 10 and numerical analyzes are performed by applying periodic boundary conditions along the vertical axis. In the numerical analysis, reflection parameters are obtained by using waveguide port. It can be observed

from the frequency dependent reflection parameters given in Figure 11 that the center operating frequency does not change when the absorber fabric is positioned on conformal structures, but the amplitude of the reflection coefficients decreases at higher frequencies.

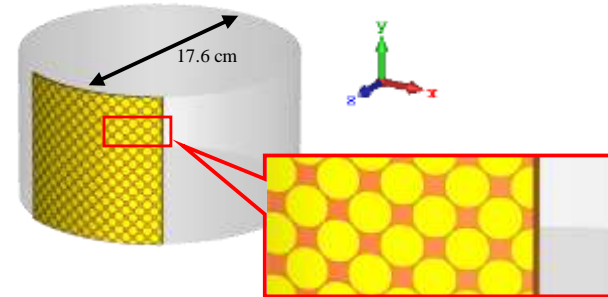


Figure 10. Radar absorber fabric placed on the curved structure

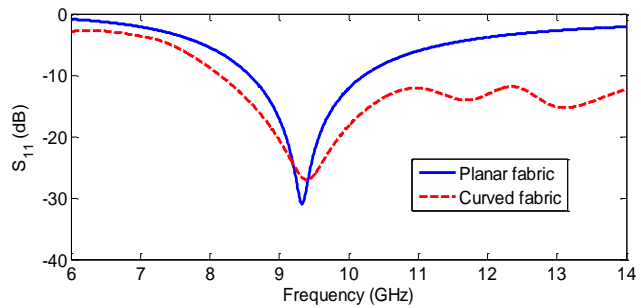


Figure 11. Comparison of the numerically obtained frequency dependent reflection coefficient values of the conformal radar absorber fabric with the planar fabric

3. Manufacturing Process and Experimental Verification

In order to experimentally verify the numerical analysis results, the prototype of the radar absorber fabric is manufactured. As schematically shown in Figure 12, the grounding conductor and circular shaped patch arrays are manufactured using conductive fabric with a shielding efficiency of 70–90 dB in the frequency range of 10 MHz –30 GHz consisting of 62% polyester, 25% copper and 13% nickel, while 1.5 mm thick neoprene fabric is used for the dielectric substrate.

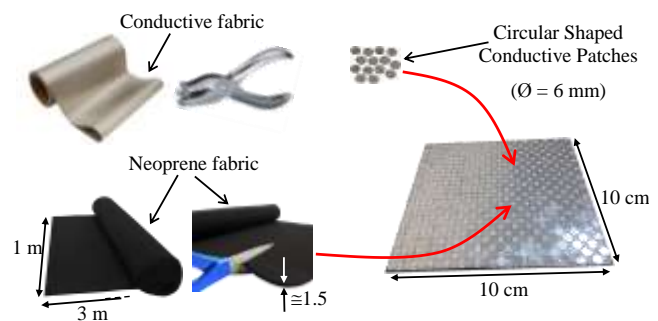


Figure 12. Prototype production stages of radar absorber fabric

After the manufacturing process is completed, the electrical performance of the radar absorber fabric is started by measuring the frequency dependent complex dielectric permittivity of the neoprene fabric. As shown in Figure 13, Agilent N5234A PNA-L microwave vector network analyzer (VNA) with an operating frequency range of 10 MHz to 43.5 GHz is used together with the Agilent 85070E dielectric measurement kit. The obtained measurement results of the neoprene fabric for the frequency range of 6–12 GHz are given in Figure 14.

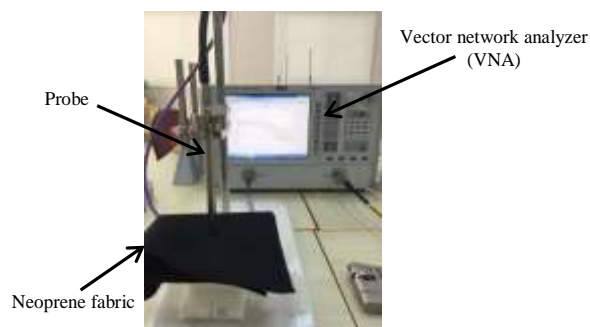
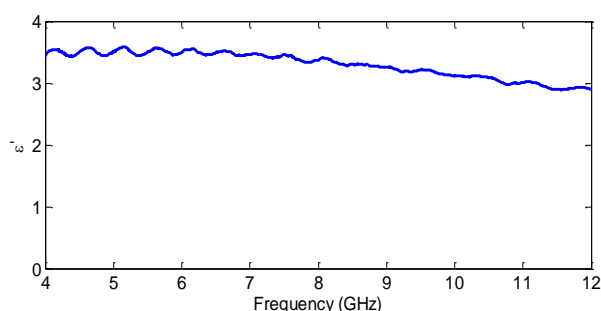
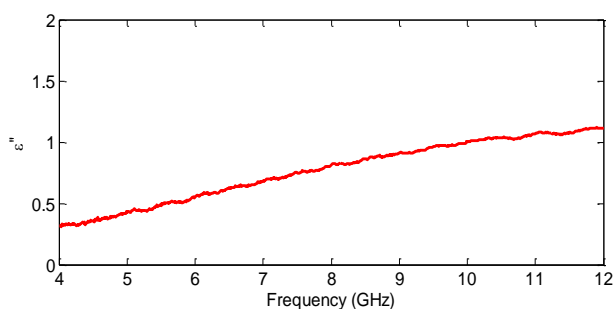


Figure 13. Measurement setup of frequency dependent complex dielectric permittivity of neoprene fabric



(a)



(b)

Figure 14. Frequency dependent complex dielectric permittivity of neoprene fabric (a) real and (b) imaginary parts

It can be observed from Figure 14 that the real and imaginary parts of the relative permittivity value of the neoprene fabric at the center operating frequency are 3.18 and 0.93, respectively. The obtained values

confirm that the electrical characteristic of the neoprene fabric is similar to the substrate used in the simulations. After the complex relative permittivity values of the neoprene fabric is verified by measurements, frequency dependent reflection coefficient values of the planar radar absorber fabric are measured. For this purpose, the free space measurement setup shown in Figure 15 is used [17]. In the measurements a horn antenna which has excellent radiation characteristics in the operating frequency range of 3 GHz to 18 GHz is located 20 cm far from the proposed structure and connected through semi rigid coaxial cable to the VNA.

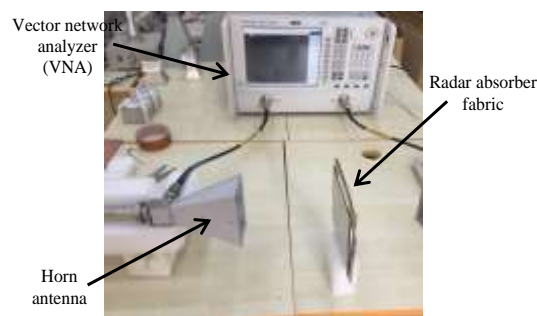


Figure 15. Frequency dependent reflection parameter measurements of planar radar absorber fabric

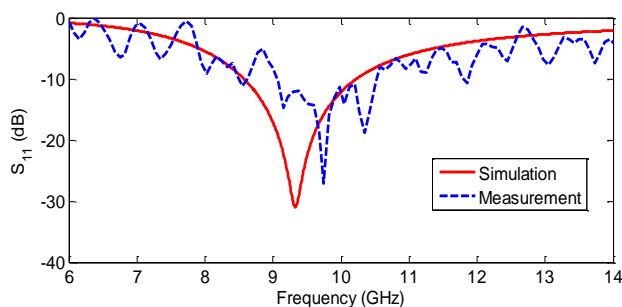


Figure 16. Comparison of the numerically obtained reflection coefficient values of the planar radar absorber fabric with the measurements

The reflection coefficient values obtained from the measurements are compared with the numerical results in Figure 16. It can be clearly seen from Figure 16 that the measurement results are consistent with the numerical results.

In order to obtain the electrical performance of the cylindrical conformal absorber fabric, as shown in Figure 17, the proposed structure is placed on a paper roll with an average radius of 8.5 cm and reflection coefficient values are obtained in the frequency range of 6-14 GHz. The reason for using a paper roll in measurements is that it has a conformal surface and has a dielectric permittivity of close to 1 which is equal to free space.

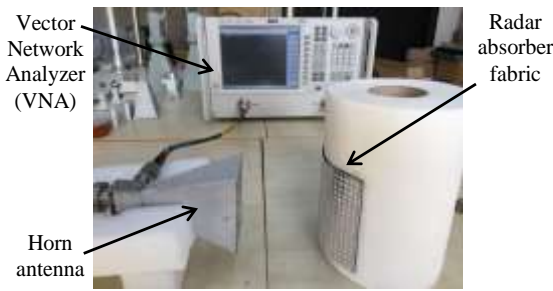


Figure 17. Frequency dependent reflection coefficient measurements of cylindrical conformal surface absorber fabric

The frequency dependent reflection coefficient values obtained from measurements are compared with the numerical analysis results in Figure 18.

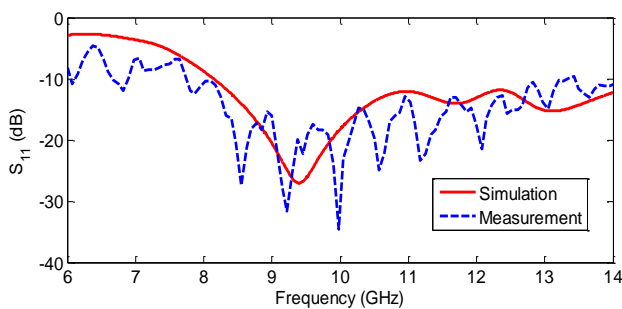


Figure 18. Comparison of the numerically obtained reflection coefficient values of the conformal radar absorber fabric with the measurements

It can be seen from the comparison given in Figure 18 that the measurement results are in good agreement with the numerical analysis results.

Finally, the electrical performance of the proposed radar absorber fabric is compared with previously published studies in terms of unit cell dimensions, material used in the manufacturing process, the operating frequency values and the polarization insensitivity. As it can be observed from Table 3, the proposed absorber represents a polarization insensitivity up to 60° and good miniaturization as well as flexibility for conformal applications.

Table 3. Electrical performance of the proposed radar absorber fabric compared with previously published studies

Ref. No.	Unit cell (mm ²)	Material	Oper. Freq. (GHz)	Pol. Insens.
[15]	30x30	Fabric	9, 9.8	0°–60°
[18]	26x26	FR4	28	0°–40°
[19]	11x11	FR4	10	Not ment.
[20]	16x16	Graph.	11.6	Not ment.
This study	8.75x8.75	Fabric	9.33	0°–60°

4. Conclusion

In this study, radar absorber fabric with a circular shaped conductive patch array which has a central operating frequency of 9.33 GHz is designed. In the designs, the electrical performance of the radar absorber fabric is numerically studied considering the different incident angle and polarization of the electromagnetic wave. In the numerical analysis, the angle of incidence of the electromagnetic wave is changed between 0°–60° with 15° angle steps. It is observed from the numerical results that the operating frequency value of the absorber fabric shifted towards high frequencies due to the increase in the incident angle whereas the operating frequency value does not change for the different polarizations of the electromagnetic wave. In order to deeply analyze the electrical performance of the radar absorber fabric 2D surface current distribution at the operating frequency value for normal electromagnetic wave excitation ($\phi=0^\circ$, $\theta=0^\circ$) is examined. Within the scope of numerical analysis, the electrical performance of the conformal structure obtained by placing the planar radar absorber fabric on the cylinder surface with an inner radius of 8.8 cm is analyzed and it is observed that the central operating frequency value has shifted 60 MHz towards the high frequency. In order to experimentally verify the numerical analysis results of both the planar and conformal radar absorber fabrics, the prototype of the proposed structure is produced, and the frequency dependent reflection coefficients are obtained by using the free space measurement technique. The measurement results of the planar radar absorber fabric are consistent with the numerical results whereas the measurement results of the cylindrical conformal radar absorber fabric are in good agreement with the numerical results. Consequently, the proposed absorber represents good miniaturization as well as flexibility for conformal applications and a polarization insensitivity up to 60° both for TE and TM modes.

Author's Contributions

Muhammet Hilmi Nisancı: Drafted and wrote the manuscript, carried out the manufacturing process of the radar absorber fabric, performed the numerical analysis.

Baha Kanberoğlu: Drafted and wrote the manuscript, performed the numerical analysis.

Yılmaz Çiğdem: Assisted the manufacturing process of the radar absorber fabric and performed the numerical analysis.

Fatih Özkan Alkurt: Performed the experiment to verify the numerical analysis results.

Muharrem Karaarslan: Supervised the experiment's progress and analysed the obtained results.

Ethics

There are no ethical issues after the publication of this manuscript.



References

- [1]. Jayalakshmi, C. G.; Inamdar, A.; Anand, A.; Kandasubramanian, B. J., 2019. Polymer matrix composites as broadband radar absorbing structures for stealth aircrafts. *Journal of Applied Polymer Science.*, 136: 1-21.
- [2]. Laws, K. E; Vesecky, J. F.; Lovellette, M. N.; Paduan, J. D. Ship tracking by HF radar in coastal waters, OCEANS 2016 MTS/IEEE Monterey; Monterey, CA, USA, 2016, pp. 1-8.
- [3]. Lee, R. J.; Steele, S. L. 2014. Military Use of Satellite Communications, Remote Sensing, and Global Positioning Systems in the War on Terror. *Journal of Air Law and Commerce*, 79(1), 69-80.
- [4]. Dzvonkovskaya, A.; Gurgel, K.; Rohling, H.; Schlick, T. Low power High Frequency Surface Wave Radar application for ship detection and tracking. 2008 International Conference on Radar; Adelaide, SA, Australia, 2008, pp. 627-632.
- [5]. Zhukov, P. A.; Kirillov, V. Y. The Use of Radar Absorbing Materials for Electronic Devices. International Youth Conference on Radio Electronics, *Electrical and Power Engineering (REEPE)*; Moscow, Russia, 2020, pp. 1-5.
- [6]. Mitrano, C.; Balzano, A.; Bertacca, M.; Flaccavento, M.; Mancinelli, R. CFRP-based broad-band Radar Absorbing Materials. IEEE Radar Conference; Rome, Italy, 2008, pp. 1-6.
- [7]. Perini, J; Cohen, L. S., 1993. Design of broad-band radar-absorbing materials for large angles of incidence. *IEEE Transactions on Electromagnetic Compatibility*, 35(2), 223-230.
- [8]. Terracher, F.; Berginc, G. Thin electromagnetic absorber using frequency selective surfaces. IEEE Antennas and Propagation Society International Symposium. Transmitting Waves of Progress to the Next Millennium. 2000 Digest. Held in conjunction with: USNC/URSI National Radio Science Meeting; Salt Lake City, UT, USA, 2000, pp. 846-849.
- [9]. Ming-liang, W.; Sheng-jun, Z.; Jia-qi, L.; Wei, L.; Xue-mei, L.; Liang, X. W. FSS design research for improving the wide-band stealth performance of radar absorbing materials. International Workshop on Metamaterials (Meta); Nanjing, China, 2012, pp. 1-4.
- [10]. Varadan, V. V. Radar Absorbing Applications of Metamaterials. IEEE Region 5 Technical Conference; Fayetteville, AR, USA, 2007, pp. 105-108.
- [11]. Lv, X.; Withayachumnankul, W.; Fumeaux, C. 2019. Single-FSS-Layer Absorber with Improved Bandwidth–Thickness Tradeoff Adopting Impedance-Matching Superstrate. *IEEE Antennas and Wireless Propagation Letters*, 18(5), 916-920.
- [12]. Xu, H.; Bie, S.; Xu, Y.; Yuan, W.; Chen, Q.; Jiang, J., 2016. Broad bandwidth of thin composite radar absorbing structures embedded with frequency selective surfaces. *Composites Part A: Applied Science and Manufacturing*, 80, 111-117.
- [13]. Bakshi, S. C.; Mitra, D. A Reconfigurable FSS Backed Continuously Tunable CAA Inspired Absorber. IEEE Indian Conference on Antennas and Propagation (InCAP); Hyderabad, India, pp. 1-4, 16-19 Dec. 2018.
- [14]. Motevasselian, A.; Jonsson, B. L. G., 2011. Partially Transparent Jaumann-Like Absorber Applied to a Curved Structure. *International Journal of Antennas and Propagation*, 2011, 1-7.
- [15]. J. Tak, J.; Choi, J., 2017. A Wearable Metamaterial Microwave Absorber. *IEEE Antennas and Wireless Propagation Letters*, 16, 784-787.
- [16]. CST Studio Suite 2019, available at www.3ds.com.
- [17]. Yan, M.; et al. 2014. A Novel Miniaturized Frequency Selective Surface with Stable Resonance. *IEEE Antennas and Wireless Propagation Letters*, 13, 639-641.
- [18]. Bilal, R. M. H; et al., 2021. Wideband Microwave Absorber Comprising Metallic Split-Ring Resonators Surrounded With E-Shaped Fractal Metamaterial. *IEEE Access*, 9, 5670-5677.
- [19]. Yoo, M.; Lim, S., 2013. Wideband metamaterial absorber using an RC layer. Asia-Pacific Microwave Conference Proceedings (APMC), 1227-1229.
- [20]. Olszewska, M., 2013. A broadband metamaterial absorbing panel with a resistive pattern made of ink with graphene nanoplatelets. European Microwave Conference, 1039-1042.

